New linear accelerator (Linac) design based on C-band accelerating structures for SXFEL facility

ZHANG Meng(张猛)[1)] GU Qiang(顾强)

Shanghai Institute of Applied Physics, Chinese Academy of Sciences, Shanghai 201800, China

Abstract: A C-band accelerator structure is one promising technique for a compact XFEL facility. It is also attractive in beam dynamics in maintaining a high quality electron beam, which is an important factor in the performance of a free electron laser. In this paper, a comparison between traditional S-band and C-band accelerating structures is made based on the linac configuration of a Shanghai Soft X-ray Free Electron Laser (SXFEL) facility. Throughout the comprehensive simulation, we conclude that the C-band structure is much more competitive.

Key words: linac, C-band, free electron laser

PACS: 29.20.Ej, 29.27.Bd, 41.60.Cr **DOI:** 10.1088/1674-1137/35/11/016

1 Introduction

Driven by the compactness of the machine, C-band technology is widely studied and seriously considered for FEL facilities. The Spring-8 Compact SASE Source (SCSS) is the first large scale facility to adopt a C-band RF structure [1] and SwissFEL [2], as well as Shanghai XFEL [3] and the Pohang Accelerator Laboratory-XFEL (PAL-XFEL) [4] is also a favored C-band for better space economy and power consumption minimization.

The SXFEL was proposed in 2006 to verify the cascaded HGHG scheme and take command of key technologies for X-Ray FEL [5]. The SXFEL linac consists of a low emittance S-band photo cathode injector, a linear accelerator with two stages of magnetic bunch compressors and one short X-band structure to linearize the compression. The nominal electron beam energy of the linac is 840 MeV, the local energy spread is 0.1%–0.15%, the peak current is about 600 A and the normalized emittance is 2 mm·mrad.

In this paper, a comparison is carried out when adopting the C-band accelerating structure for SXFEL instead of the traditional S-band after BC2, for the A3 section as shown in Fig. 1. To effectively compensate for the energy spread that is introduced in A2, four 3-m SLAC type accelerating structures are applied instead of six in the initial design [6]. Under the influence of a higher field gradient and stronger longitudinal wakefield of the C-band RF structure, the simulation results show that the accelerating efficiency and the stability of the whole machine are much better than with the S-band option. A physical understanding of the beam dynamics is presented.

This paper is organized as follows. First the background and SXFEL linac are described, and the model for comparison is given. The higher efficiency of the C-band structure is shown in the next section (part 2). The tracking results from start to end (S2E) simulation are also presented. The jitter studies focus mainly on the longitudinal dynamics, since the FEL process is more sensitive to the longitudinal planes than the transverse planes. Part 3 gives a compari-

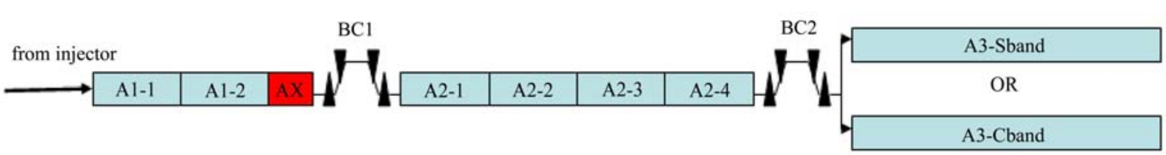

Fig. 1. The SXFEL layout for the comparison of the S-band and C-band accelerating structures after BC2.

Received 11 January 2011, Revised 16 February 2011

1) E-mail: zhangmeng@sinap.ac.cn

son for jitter tolerance control when the C-band is used. Finally, a brief outlook and the conclusion are given at the end.

2 Compactness and efficiency comparisons

To achieve a high peak current and small energy spread at the exit of the linac, the bunch must be compressed using two magnetic chicanes, BC1 and BC2 as shown in Fig. 1. The non-linearities in the compression and acceleration process can be mostly canceled using the X-band structure AX. The semi-analytic fast code Litrack is applied to choose the acceleration and compression parameters in order to provide the desired FEL beam [7]. An accelerator design for a 0.5-nC bunch charge is described here, as shown in Fig. 2. The energy spread induced upstream of the magnetic chicane is well compensated using off-crest acceleration, and it is affected by the longitudinal wakefield of the A3 section.

When the C-band accelerating structure is adopted for the A3 section, the results compared with the S-band RF structures are shown in Table 1. The results are also presented when the SLAC Energy Doubler (SLED) is switched on for this section. Shorter wavelength and stronger impedance make the C-band option compensate for the energy spread effectively at the off crest 28°, much less than the S-band 50° off crest acceleration. This can significantly increase the machine efficiency, and a higher field gradient can also come from the inherent C-band advantage.

Under the C-band design, the accelerating structure is 23 m, one third of the total length compared with the S-band main linac accelerating structure. When the SLED is applied for the power supplies, the total length is reduced further, although the

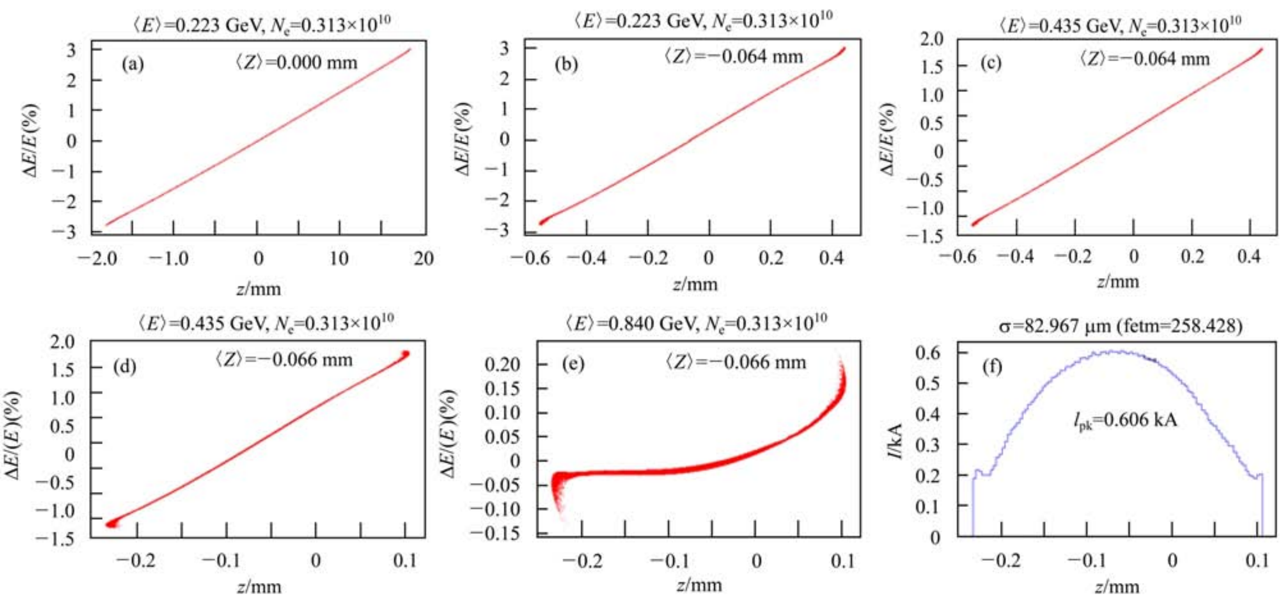

Fig. 2. The longitudinal phase space after X-band linearization (a), after the first chicane BC1 (b), before (c) and after (d) the second chicane BC2. The phase space (e) and the beam current profile (f) at the exit of the linac.

Table 1. A comparison of results from S-band and C-band operation for the A3 section (the result when sled is switched on is shown in brackets).

		S-band (with SLED)	C-band (with SLED)
beam parameter	energy/GeV	> 0.84	
	energy spread/rms	< 0.1%	
	peak current/A	> 600	
total length/m		35 (26)	23(12.5)
gradient/(MV/m)		18 (18×1.5)	20 (20×2)
off crest/(°)		50 (55)	28 (35)

accelerating phases are not close to the crest because of the reduced wakefield from the shortened accelerating structure. To keep the results comparable at the same level, the beam parameters at the exit are adjusted to the same required specifications in our simulation.

For the C-band scenario, S2E simulation has been done and the slice emittance alone of the bunch is well controlled below 1 mm·mrad as shown in Fig. 3. The FEL requirements for slice energy spread and beam current are also achievable.

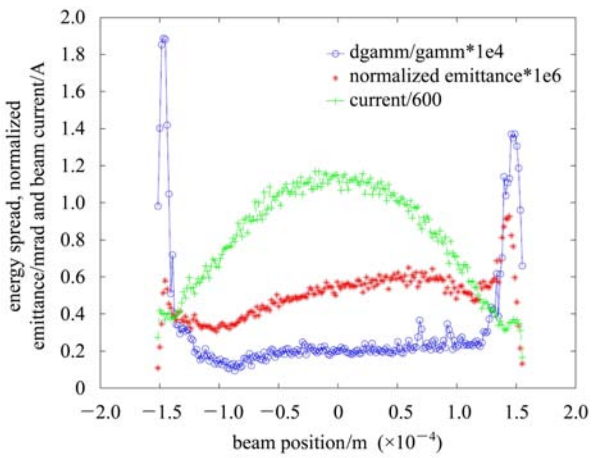

Fig. 3. The slice normalized emittance, the slice energy spread and the beam current at the end of the accelerator.

3 Tolerance budget comparisons

Table 2 lists the sensitivities for RF phase, RF voltage, and chicane bend power supplies the various systems. The sensitivity for each system causes a 0.1% relative electron energy increase. These sensitivities will be used to form a tolerance budget based on random summing. In this paper, only A3 is studied under the influence of the frequency of RF structures, so the peak current and arrival time jitter are always unchanged because of the ultra relative beams. As for the average energy, the jitter from the phase jitter can be expressed as $\Delta E/E_0=-\text{tg}\varphi_0\cdot\Delta\varphi$. For the C-band option, the phase jitter from the power source can be more effectively controlled because of the less off-crest accelerating phase. As shown in Table 2, we also give the results for three different typical compress factor configurations of the magnetic chicane. Compared with the S-band option, the C-band RF structure has an obvious advantage in jitter control, regardless of different compress factor distributions. The simulation results also suggest that a stronger compression for the first chicane is favored for the stability of the linac.

Table 2. Tolerance budget for the S-band and C-band without SLED.

parameter	symbol	$\Delta E/E$=0.1% compress factor: 2×6 4×3 6×2 S-band	C-band	unit
mean L1 RF phase	φ1	0.098	0.112	°
		0.114	0.128	
		0.120	0.149	
mean Lx RF phase	φx	5.431	5.903	°
		6.199	6.794	
		6.625	7.861	
mean L2 RF phase	φ2	0.184	0.205	°
		0.370	0.394	
		0.633	0.688	
mean L3 RF phase	φ3	0.073	0.169	°
		0.100	0.226	
		0.118	0.299	
mean L1 RF voltage	$\Delta V1/V1$	0.121	0.139	%
		0.141	0.159	
		0.149	0.187	
mean Lx RF voltage	$\Delta Vx/Vx$	0.635	0.728	%
		0.786	0.882	
		0.829	1.034	
mean L2 RF voltage	$\Delta V2/V2$	0.088	0.098	%
		0.176	0.188	
		0.240	0.262	
mean L3 RF voltage	$\Delta V3/V3$	0.203	0.204	%
		0.206	0.206	
		0.204	0.205	
BC1	$\Delta R56/R56$	0.2365	0.2794	%
		0.1720	0.1990	
		0.1635	0.2142	
BC2	$\Delta R56/R56$	0.1113	0.1282	%
		0.3100	0.3500	
		0.6204	0.7835	
gun timing jitter	$\Delta t0$	0.581	0.580	ps
		0.791	0.794	
		0.860	0.858	
initial bunch charge	$\Delta Q/Q0$	11.489	11.713	%
		17.721	16.357	
		17.950	17.050	

4 Conclusions

The accelerating efficiency and stability of the C-band structure machine are much better than those of the S-band option. The C-band RF system R&D in SINAP has started, aiming at building the accelerating structures with a constant gradient of higher than 40 MV/m [8]. The advantage of the C-band operation after the second magnetic chicane is obvious as shown in this study. For further A2 section C-band operation, especially for the compactness of the future hard X-ray FEL facility, beam dynamics should be studied not only in longitudinal phase space, but also in transverse phase space in terms of the longer bunch length and also the stronger transverse wakefield before the compressor.

References

1 Shintake T. Status Report on Japanese XFEL Construction Project at SPring-8. In: Proceedings of IPAC 2010. Kyoto, Japan, 2010

2 Reiche S. The SwissFEL X-Ray Free Electron Laser. In: Candle-DESY-PSI collaboration workshop. Candle, Yerevan, Armenia, 2010

3 FENG C. Design Studies of Shanghai Hard XFEL. In: EFST workshop on Compact X-ray Free-Electron Lasers. Shanghai, China, 2010

4 LEE T Y, BaE Y S, CHOI J et al. Journal of the Korean Physical Society, 2006, **48**: 791–795

5 CHEN Jian-Hui, DENG Hai-Xiao, GU Qiang et al. Chinese Physics C (HEP & NP), 2009, **33**(8): 706–710

6 YAN Jun, ZHANG Meng, DENG Hai-Xiao et al. Nuclear Instruments and Methods in Physics Research A, 2010, **615**(3): 249–253

7 Bane K L F, Emma P. Litrack: A Fast Longitudinal Phase Space Tracking Code with Graphical User Interface. In: Proceedings of PAC 2005, Knoxville, Tennessee, USA, 2005

8 ZHAO Z T. Progress in SDUV-FEL and Development of X-ray FELs in Shanghai. In: Proceedings of FEL 2010, Hilton Malmo City, Sweden, 2010